Digital Communications and Networks 11 (2025) 2016–2029

Contents lists available at ScienceDirect

Digital Communications and Networks

journal homepage: www.keaipublishing.com/dcan

Resource allocation for AI-native healthcare systems in 6G dense networks using deep reinforcement learning ☆

Jianhui Lv [a,*], Chien-Ming Chen [b], Saru Kumari [c], Keqin Li [d]

[a] Multi-modal Data Fusion and Precision Medicine Laboratory, The First Affiliated Hospital of Jinzhou Medical University, Jinzhou 121012, China
[b] School of Artificial Intelligence, Nanjing University of Information Science & Technology, Nanjing 210044, China
[c] Department of Mathematics, Chaudhary Charan Singh University, Meerut, India
[d] Department of Computer Science, State University of New York, New Paltz, NY 12561, USA

ARTICLE INFO

Keywords:
Resource allocation
AI-native healthcare systems
6G dense networks
Deep reinforcement learning

ABSTRACT

Although 6G networks combined with artificial intelligence present revolutionary prospects for healthcare delivery, resource management in dense medical device networks stays a basic issue. Reliable communication directly affects patient outcomes in these settings; nonetheless, current resource allocation techniques struggle with complicated interference patterns and different service needs of AI-native healthcare systems. In dense installations where conventional approaches fail, this paper tackles the challenge of combining network efficiency with medical care priority. Thus, we offer a Dueling Deep Q-Network (DDQN) -based resource allocation approach for AI-native healthcare systems in 6G dense networks. First, we create a point-line graph coloring-based interference model to capture the unique characteristics of medical device communications. Building on this foundation, we suggest a DDQN approach to optimal resource allocation over multiple medical services by combining advantage estimate with healthcare-aware state evaluation. Unlike traditional graph-based models, this one correctly depicts the overlapping coverage areas common in hospital environments. Building on this basis, our DDQN design allows the system to prioritize medical needs while distributing resources by separating healthcare state assessment from advantage estimation. Experimental findings show that the suggested DDQN outperforms state-of-the-art techniques in dense healthcare installations by 14.6% greater network throughput and 13.7% better resource use. The solution shows particularly strong in maintaining service quality under vital conditions with 5.5% greater QoS satisfaction for emergency services and 8.2% quicker recovery from interruptions.

1. Introduction

Combining 6G networks with artificial intelligence-native healthcare systems signals a revolutionary change in medical service delivery [1–3]. AI-native healthcare systems, defined by their natural integration of artificial intelligence for medical data processing, diagnosis support, and treatment optimization, call for unmatched degrees of network performance [4]. From real-time patient monitoring to high-resolution medical imaging, these systems handle enormous volumes of healthcare data, demanding ultra-reliable and low-latency connectivity. Supporting communication between Medical Devices (MD) and Artificial Intelligence (AI) in a bidirectional manner that improves both network optimization and healthcare service quality, the 6G Dense Network (DN) architecture becomes a key enabler for these sophisticated healthcare applications [5–7].

As healthcare institutions deploy more and more AI-powered sensors and devices [8,9], the density of network nodes rises dramatically. As recorded in recent healthcare IoT studies [10], a modern hospital ward can include hundreds of connected devices per room. Operating rooms often have 30 to 50 networked devices, including surgical robots, imaging systems, and anesthesia equipment; intensive care units usually have 15 to 20 monitoring devices per bed (patient monitors, ventilators, infusion pumps). Depending on the severity, emergency departments have different device densities; trauma rooms may have up to 35 linked devices in a 25 m^2 space. Healthcare institutions are using more AI-enhanced equipment for better patient care, which is driving this density

☆ Peer review under the responsibility of the Chongqing University of Posts and Telecommunications.

* Corresponding author at: The First Affiliated Hospital of Jinzhou Medical University, Jinzhou 121012, China.
E-mail addresses: lvjianhui2012@163.com (J. Lv), chienmingchen@ieee.org (C.-M. Chen), saryusiirohi@gmail.com (S. Kumari), lik@newpaltz.edu (K. Li).

https://doi.org/10.1016/j.dcan.2025.06.011
Received 26 February 2025; Received in revised form 5 June 2025; Accepted 22 June 2025

Available online 27 June 2025

to rise. This extensive distribution creates notable interference issues that could compromise the reliability of vital medical services [11]. Often relying on static optimization methods, conventional resource allocation policies struggle to control the complex interference patterns in crowded medical environments. The healthcare environment increases even more complexity from delay-sensitive emergency communications to bandwidth-intensive medical imaging transfers since different medical uses have varying priority and Quality of Service (QoS) requirements.

The intersection of AI-native healthcare systems with 6G DN raises unique resource allocation problems outside conventional network optimization considerations [12,13]. Medical equipment must meet strict performance promises in busy hospital environments while sharing a restricted spectrum of resources. For instance, whereas artificial intelligence-powered surgical robots require ultra-reliable communication connections with minimal interference, patient monitoring systems demand continuous data collecting by constant connectivity. Therefore, the resource allocation system must consider several services' technical network elements, medical criticality, and specific performance requirements [14].

Ineffective resource allocation in real healthcare settings produces observable effects. For instance, transmission delays over 200 ms in surgical settings can interfere with robotic surgery systems, increasing patient danger and perhaps prolonging operations by 15 to 20 minutes for each incident. Patient monitoring data streams in intensive care units call for constant 99.999% dependability since every 0.1% drop in transmission reliability corresponds to roughly 12 missed crucial warnings every day per ward. Diagnostic imaging transfers are delayed more than 30 seconds because of network congestion, which also increases typical diagnosis times by 17 minutes, impacting patient treatment schedules and hospital throughput directly [15].

Previous research has examined several resource allocation techniques in dense networks [16,17]. While some studies on power control and resource block assignment strategies have emphasized interference-aware matching theory for device-to-device communications, others have emphasized these approaches. However, the dynamic nature of medical operations and the different requirements of numerous healthcare applications create a more complex optimization landscape, which often fails in AI-native healthcare settings. When one considers the need to maintain the Quality of Experience (QoE) for medical professionals while ensuring patient safety through continuous network performance [18], the problem becomes extremely challenging.

Three separate types may be used to categorize earlier studies on resource allocation. Wang et al. [19] conducted substantial research on but were not created with healthcare-related limits in mind. However, there is no consideration for prioritizing medical data. Wu and He [20] present self-learning networks that improve security in AI-enabled systems. Although not addressing communication resource management, healthcare-focused strategies have surfaced lately, such as Long et al. [21] using artificial intelligence in healthcare supply chains. While Jagannath et al. [22] proposed an IoT-enabled smart healthcare system using deep reinforcement learning. Their method, however, depends on simplified interference models inappropriate for dense medical device installations. In healthcare settings, these current studies show three shared shortcomings: they usually presume consistent service needs across all network nodes, seldom include medical criticality in their optimization goals, and poorly handle the rigorous reliability expectations where even transient communication failures could affect patient care.

Accordingly, the main contributions of this paper are summarized as follows:

- We introduce a point-line graph coloring interference model specifically designed for healthcare environments.
- We develop a healthcare-aware DDQN architecture that separates state value estimation from advantage calculation, enabling more precise evaluation of resource allocation decisions in medical contexts.
- We create an adaptive learning framework that autonomously generates resource allocation strategies tailored to healthcare environments.

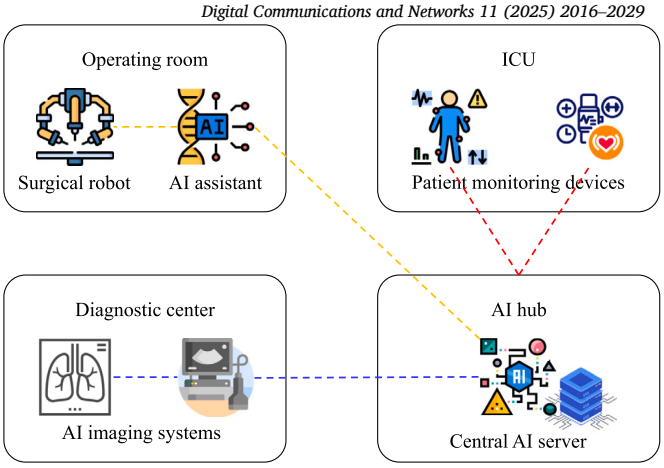

Fig. 1. AI-native healthcare system in 6G dense network.

The rest of the paper is organized as follows. Section 2 introduces the system model. Section 3 presents the healthcare network interference model based on point-line graph coloring and develops the healthcare-aware resource allocation strategy. Section 4 details the deep reinforcement learning approach, introducing the healthcare-aware DQN resource allocation model and the specialized DDQN algorithm for medical network optimization. Section 5 provides the experiments and results analysis. Finally, Section 6 concludes the paper.

2. System model

This study examines an advanced medical communication scenario within 6G DN, illustrated in Fig. 1, where AI-native healthcare systems enable intelligent medical services, automated diagnostics, and real-time patient monitoring. The network infrastructure supports critical medical operations through a distributed system of $\mathcal{H}$ healthcare nodes forming $\mathcal{K}$ medical communication links. The medical network environment integrates multiple components: AI-enabled diagnostic systems ($\mathcal{D}$), patient monitoring devices ($\mathcal{P}$), robotic surgical equipment ($\mathcal{S}$), and emergency response units ($\mathcal{E}$). This healthcare-oriented network achieves bidirectional intelligence enhancement through the collaboration between medical artificial intelligence ($\mathcal{M}$) and communication systems ($\mathcal{C}$). As medical smart terminals ($\mathcal{T}$) become increasingly prevalent and healthcare networks expand rapidly, conventional 5G DN architectures cannot fully meet the rising technical requirements for autonomous operation, ultra-large scale deployment, highly dynamic adaptation, and complete intelligence in medical service delivery. The anticipated growth in smart healthcare systems and internet of medical things devices may exceed current 5G DN capabilities. In comparison, 6G DN healthcare implementations will support 10 times higher network capacity for medical data transmission and one-tenth the latency for critical procedures while serving 10 times more medical terminal devices and ensuring enhanced quality of medical service. We establish a point-line graph coloring approach for modeling overlapping interference patterns between healthcare nodes to optimize resource allocation in this complex medical network topology.

2.1. Network coverage model and 6G DN healthcare topology

Modern healthcare operations depend on complex interconnection structures created by creating communication coverage zones and net-

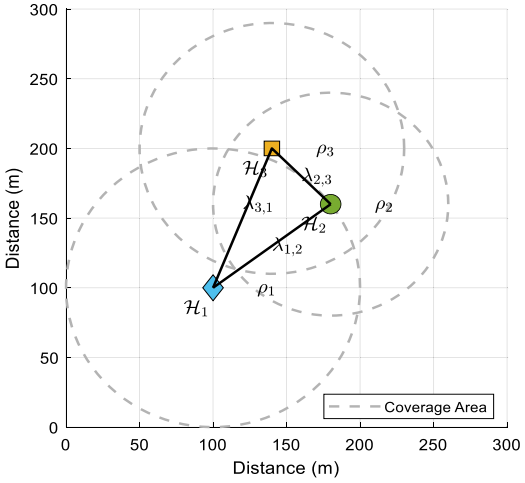

Fig. 2. Healthcare device coverage and communication links.

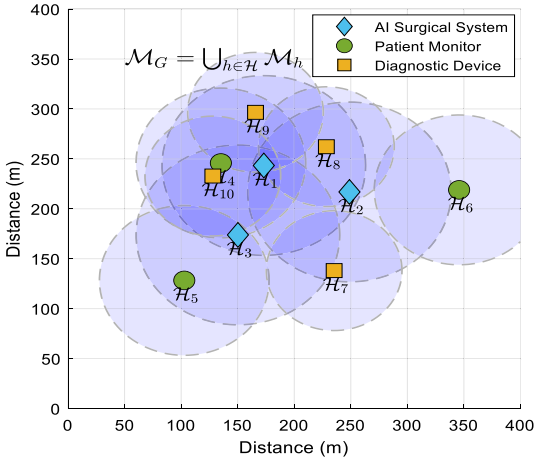

Fig. 3. Healthcare network coverage model.

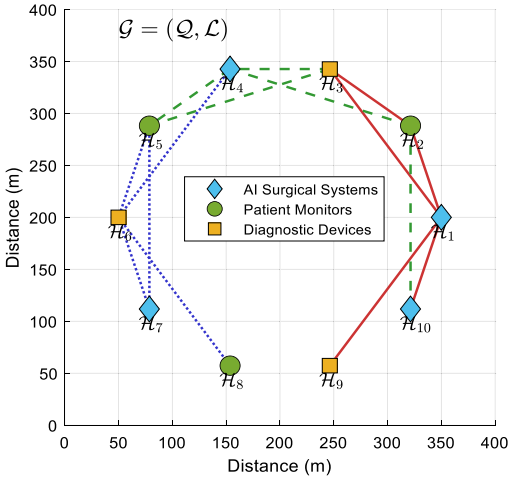

Fig. 4. Healthcare network topology.

work topology patterns in advanced medical settings. Providing several medical services—from real-time patient monitoring to emergency response systems—helps create this complexity. When analyzing the medical network configuration between three fundamental healthcare devices ($\mathcal{H}_1$, $\mathcal{H}_2$, and $\mathcal{H}_3$) within a smart hospital environment as shown in Fig. 2, we observe that each medical device functions within a carefully orchestrated wireless coverage domain that overlaps with its neighboring devices. For critical medical operations, this overlapping coverage guarantees redundancy and ongoing connectivity. Following exact healthcare-specific distance standards, dependable connectivity is preserved while reducing any interference that might compromise medical service quality, and medical communication networks between healthcare equipment follow. Maintaining continuous healthcare service delivery depends on carefully balancing coverage and interference control.

$$\lambda_{m,n} \leq \min(\rho_m, \rho_n) \tag{1}$$

where $\lambda_{m,n}$ represents the Euclidean distance between medical devices $\mathcal{H}_m$ and $\mathcal{H}_n$, while ρ_m and ρ_n denote their respective medical service coverage radii. Real-world medical environments introduce device heterogeneity, leading to $\rho_m \neq \rho_n$ due to varying healthcare application requirements.

In Fig. 3, we observe how medical devices in a hospital facility create a synergistic web of service coverage. The illustration shows how different medical devices perform in perfect unison so that healthcare services can be rendered throughout the institution. The whole medical service coverage area $\mathcal{M}_\mathcal{G}$, which marks the extent of medical service area coverage, is defined by the mathematical union of individual device coverage zones, thus ensuring critical operational geospatial coverage for major healthcare services. The integration of coverage zones ensures continuous availability of healthcare services throughout hospital regions, including but not limited to emergency rooms and patient care units.

$$\mathcal{M}_G = \bigcup_{h\in\mathcal{H}} \mathcal{M}_h \tag{2}$$

where $\mathcal{M}_h$ indicates the coverage zone of medical device h, and $\mathcal{H}$ encompasses all healthcare devices in the facility. This unified coverage model ensures seamless medical service delivery across the entire healthcare environment.

Visualized in Fig. 4, the resulting healthcare network topology shows an integration of medical services using a customized mathematical graph structure that catches the intricate interactions between various healthcare equipment and their communication paths. Using exact modeling of how medical equipment interacts and exchanges resources within the hospital setting, this graph-based representation forms a complete framework supporting several healthcare activities ranging from routine patient monitoring to emergency care coordination.

$$\mathcal{G} = (\mathcal{Q}, \mathcal{L}) \tag{3}$$

where $\mathcal{Q} = 1, 2, \ldots, \mathcal{N}$ denotes the set of healthcare devices, and $\mathcal{L} = 1, 2, \ldots, \mathcal{K}$ represents the set of medical communication links. From regular patient monitoring to emergency medical responses, this architecture fits many healthcare environments while preserving AI-driven service quality enhancement. The network topology allows real-time medical data transfer, AI-assisted diagnosis, and automated treatment coordination using dense deployment of linked healthcare devices. Every medical gadget function as a network node and a data collecting point, therefore adding to the general dependability and effectiveness of the healthcare communication system.

2.2. Resource allocation in healthcare 6G DN

The resource allocation technique in AI-native healthcare networks shows a clever way to maximize communication resources across medical device linkages, reflecting congruence with the complex network architecture shown in Fig. 4. This optimization strategy meticulously analyzes numerous aspects essential to healthcare operations, from emergency response systems to routine patient monitoring and the intricate interactions between connected medical equipment, including the distinct objectives of various medical services. Aiming to minimize inter-

ference between simultaneous medical procedures, the allocation mechanism guarantees ongoing healthcare service delivery by means of an advanced decision-making system that methodically distributes communication resources. The system considers long-term service quality criteria with urgent operational needs to optimize resource allocation and maintain optimal performance. Using a mathematical formulation that includes both the technical limitations and medical service priority for any two medical devices sharing network access points, we can define this healthcare-aware resource allocation goal as:

$$\begin{aligned} &\min \sum_{\alpha\in\mathcal{A}} \sum_{\beta\in\mathcal{A}} \omega(\alpha,\beta) \\ &\text{s.t. } \xi_\alpha \cap \xi_\beta = \varnothing, \alpha \neq \beta \end{aligned} \tag{4}$$

where $\omega(\alpha,\beta)$ represents the medical resource relationship between communication links α and β, taking a value of $\omega(\alpha,\beta)=1$ when the links share identical medical communication resources, and $\omega(\alpha,\beta)=0$ otherwise. The constraint $\xi_\alpha \cap \xi_\beta = \emptyset$ guarantees that connections α and β in the healthcare network architecture do not share common medical equipment. From real-time surgical data transmission to continuous patient monitoring, this formulation covers several medical situations and guarantees the best use of resources across several healthcare uses. The allocation approach considers the density of device deployment and the criticality of medical services, so adjusting resource allocation depends on network circumstances and medical procedure needs. For instance, although patient monitoring devices use resource-sharing systems when suitable, artificial intelligence-assisted surgical systems get priority resource allocation to keep ultra-reliable communication. While keeping the rigorous performance criteria of medical applications, this healthcare-aware method guarantees effective spectrum use.

A multi-level adjustment system allows the resource allocation framework to vary with real-time medical scenario fluctuations. The system tracks three important network-level metrics at 100 ms intervals: Link Quality Indicators (LQI) for all medical connections, queue status for various service kinds, and device mobility patterns. The system activates instant resource reallocation when LQI values fall below-specified thresholds—varying by service type: 20 dB for emergency services, 15 dB for surgical systems, and 10 dB for monitoring devices. The allocation mechanism raises resource assignment by 20-40% depending on medical priority for service queues over 75% capacity. Device mobility causes reallocation when movement surpasses 2 meters for stationary equipment or 5 meters for mobile devices. This multi-parameter monitoring guarantees that resources follow the real demands of medical operations as they change.

There are many pragmatic constraints on the system model. First, the model presumes ideal Channel State Information (CSI), which could not be accessible in healthcare settings because of sensing constraints and fast-changing circumstances. This can lower allocation efficiency by 8 to 12% in very volatile environments. Second, the model struggles with a basic trade-off between reliability promises and resource use. By setting aside 15% of available resources for emergency services, our approach prioritizes dependability, guaranteeing vital service availability despite declining general network efficiency. Third, in extremely dense deployments >500 devices/km^2, the computational needs for best allocation rise dramatically, requiring approximation approaches that give up 5-7% of the performance for tractability. These limitations must be carefully controlled when putting the technology in actual healthcare settings.

3. AI-native healthcare network interference model

3.1. Healthcare network interference model using graph coloring

Effective resource allocation in the complicated context of dense healthcare networks depends on a thorough awareness of the complex interference patterns that develop across many medical devices, from surgical equipment to critical care monitoring. The administration of these resources calls for a creative strategy that considers the special needs of medical services as well as the technological features of wireless communications. We construct a specific association matrix $\mathcal{B}_M$ that properly captures and quantifies the many interactions between healthcare equipment and their accompanying communication channels to approach this difficulty methodically. Under this design, the medical device network of $\mathcal{N}$ healthcare devices, each with particular medical use, and $\mathcal{K}$ medical communication links enable data exchange among these devices. The Euclidean distance between two medical devices μ_i and μ_j defines their spatial connection, sometimes known as $\phi_{i,j}$. The determination of connectivity feasibility depends critically on this distance measure; when $\phi_{i,j}$ meets the connection conditions described in equation (1), the devices μ_i and μ_j can create a safe medical data link, therefore facilitating important healthcare information exchange.

We validate the point-line graph coloring interference model using communication traces collected from three hospital environments over six months. The dataset includes transmission patterns from 28 medical device types, including telemetry monitors, infusion pumps, ventilators, and surgical navigation systems. Analysis reveals that medical devices exhibit unique communication patterns characterized by (1) Periodic reporting intervals with strict timing requirements, (2) Burst transmissions during clinical events, and (3) Redundant transmission paths for critical data. Our model is calibrated to account for these patterns, with particular attention to the co-existence requirements of life-critical systems.

We formally depict these intricate device connections and their communication patterns using the association matrix of the healthcare network using $\mathcal{B}_M^T$, therefore offering a mathematical framework for resource allocation decision analysis and optimization. This matrix provides a framework for interference control and resource optimization and captures the network's whole connection topology.

$$\mathcal{B}_M^T = \begin{bmatrix} \beta_{1,1} & \cdots & \beta_{1,\mathcal{N}} \\ \vdots & \beta_{\alpha,\mu} & \vdots \\ \beta_{\mathcal{K},1} & \cdots & \beta_{\mathcal{K},\mathcal{N}} \end{bmatrix} \tag{5}$$

Effective resource allocation in dense healthcare settings requires a sophisticated methodology that thoroughly examines the complex network of interactions among many medical equipment. We have created a specific association matrix $\mathcal{B}_M$ to provide a complete mathematical framework for encapsulating and evaluating the many interactions between medical equipment and their communication channels. Our healthcare network design consists of $\mathcal{N}$ healthcare devices, including critical care monitors, surgical equipment, and patient monitoring systems, together with $\mathcal{K}$ medical communication lines that enable important data interchange as shown in Fig. 5. The Euclidean distance [23] $\phi_{i,j}$ exactly measures the spatial relationships between any pair of medical equipment μ_i and μ_j. This is essential for deciding if medical data transmission is feasible and of quality. While preserving the high dependability standards of healthcare communications, this distance metric guarantees the best deployment and connectivity of medical devices.

In medical device networks, each communication link plays a specific and dedicated role in connecting exactly two healthcare devices to enable critical data exchange. For example, this could involve establishing a secure, high-bandwidth connection between a surgical robot and its associated medical imaging system or linking a patient monitoring device to its central data processing unit. This one-to-two relationship constraint ensures focused, reliable communication pathways and can be mathematically expressed as:

$$\sum_{\mu\in\mathcal{M}} \beta_{\alpha,\mu} = 2, \forall \alpha \in \mathcal{A} \tag{6}$$

The interference experienced by an individual medical device can be quantified through:

$$\theta_\mu = \frac{1}{2\kappa_\mu} \sum_{\alpha\in\mathcal{A}_\mu} \sum_{\alpha'\in\mathcal{A},\alpha'\neq\alpha} \omega(\alpha,\alpha') |\xi_\alpha^T \xi_{\alpha'}| \tag{7}$$

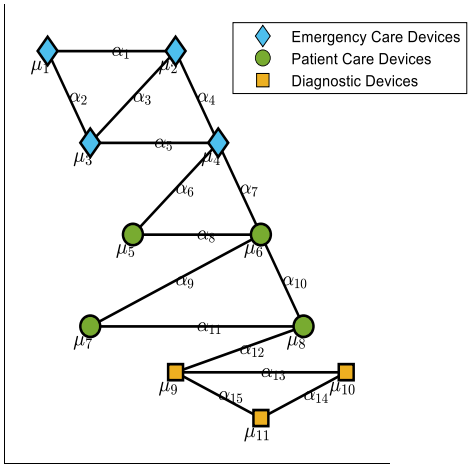

Fig. 5. Healthcare network undirected graph model.

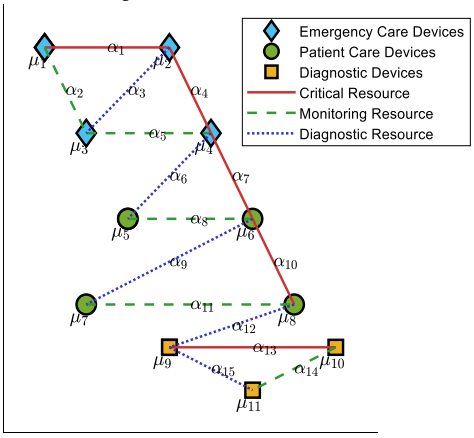

Fig. 6. Healthcare network resource allocation state.

where θ_μ represents the interference level at medical device μ, $\mathcal{A}_\mu$ denotes the set of communication links containing device μ, κ_μ indicates the number of links used by device μ, and ξ_α^T represents the transpose of ξ_α.

We select the Euclidean distance metric for modeling spatial relationships between medical devices. In controlled healthcare environments, signal propagation follows predominantly line-of-sight paths where Euclidean distance accurately predicts signal strength. Additionally, unlike Manhattan distance, which overestimates separation in open hospital spaces, or Minkowski distance metrics, which require additional parameter tuning, Euclidean distance provides a balanced approximation of actual signal paths.

The overall healthcare network interference can be calculated by aggregating individual device interference levels:

$$\theta_M = \frac{1}{\mathcal{K}} \sum_{\mu \in \mathcal{M}} \kappa_\mu \theta_\mu \tag{8}$$

To demonstrate how our interference model functions in real healthcare environments, we examine a practical scenario involving medical device μ_6, representing a central patient monitoring system utilizing multiple communication links to interact with various medical sensors and data processing units. The interference level experienced by this device, which directly impacts the reliability of patient data transmission and monitoring quality, can be systematically calculated through the following mathematical expression:

$$\begin{aligned}
\theta_6 &= \frac{1}{2\kappa_6} \sum_{\alpha \in \mathcal{A}_6} \sum_{\alpha' \in \mathcal{A}, \alpha' \neq \alpha} \omega(\alpha, \alpha') |\xi_\alpha^T \xi_{\alpha'}| \\
&= \frac{1}{2 \times 4} \sum_{\alpha \in \mathcal{A}_6} \sum_{\alpha' \in \mathcal{A}, \alpha' \neq \alpha} \omega(\alpha, \alpha') |\xi_\alpha^T \xi_{\alpha'}| \\
&= \frac{1}{8} ([1]^T [1]) \\
&= \frac{1}{4}
\end{aligned} \tag{9}$$

where $\theta_6 = \frac{1}{4}$ indicates that device μ_6 experiences interference in one-fourth of its communication links.

What strategies are appropriate for assessing interference patterns in a sophisticated healthcare network? Focusing on the role of each medical device in the interference to which it contributes, some level of interference can be advantageous and, in other instances, detrimental to the quality of care received by the patient and the service offered. In Fig. 6, we can portray a representative case study using the medical device μ_6, which acts as a central monitoring station, serving patient monitors, diagnostic devices, and emergency response units through multiple communicational links with interfaces and coprocessors. The multifaceted connections of this device introduce a myriad of possible interference patterns to be managed to deliver quality healthcare services.

The total network interference for this healthcare configuration can be expressed as:

$$\theta_M = \frac{1}{\mathcal{K}} \sum_{\mu \in \mathcal{M}} \kappa_\mu \theta_\mu = \frac{1}{15} (4 \times \frac{1}{4} + 4 \times \frac{1}{4}) = \frac{2}{15} \tag{10}$$

The formulation establishes a solid framework for measuring and analyzing complex interference patterns in healthcare networks, allowing for optimized resource allocation across various medical applications with differing levels of criticality. The model integrates advanced weighting mechanisms that consider the specific needs and priorities of various medical devices in the hospital setting. While balancing resources for regular patient monitoring devices that can handle more flexible performance criteria, it gives interference management for vital surgical systems needing ultra-reliable, low-latency communication priority. Including healthcare-specific factors into the mathematical model guarantees consistent communication channels for medical services, including long-term patient monitoring systems gathering continuous health data and emergency response systems needing quick data transfer. By means of interference quantification, the network can maintain the best performance across healthcare activities, enabling effective medical service delivery and enhancing the quality of patient care.

The computational complexity of interference calculations presents implementation concerns in large-scale healthcare networks. For a network with N medical devices and K communication links, the worst-case time complexity for constructing the complete interference model is $O(K^2)$, as each link must be evaluated against all others. For dense deployments with hundreds of devices, we implemented three optimization techniques: (1) A spatial partitioning algorithm that limits interference calculations to geographically proximate devices, reducing complexity to $O(K \log K)$ in typical hospital layouts; (2) A caching mechanism that stores interference patterns for static devices and only updates calculations for mobile elements; and (3) A parallel computation framework that distributes calculations across multiple cores, achieving near-linear speedup on our test platform.

3.2. Healthcare-aware resource allocation strategy

The integrated healthcare communication system needs sophisticated and dynamic interference control capabilities to guarantee dependable operation among a dense network of linked medical devices during medical network construction and evolution. Applying Eq. (10) to actual clinical settings allows us to methodically assess and measure interference levels resulting from the complex interactions among

several medical devices, including patient monitors, surgical tools, and diagnostic systems, all closely adjacent.

Achieving a condition whereby $\theta_M = 0$ marks a significant turning point in the framework of AI-native healthcare networks as it indicates that the system has effectively distributed resources in a way that removes negative interference among medical devices. In healthcare environments where any communication disturbance might affect patient care quality or important medical operations, this interference-free situation is essential.

From its starting condition, where devices may experience different degrees of interference, the resource allocation strategy for medical applications follow a well-organized progression, transforming the network from its current state to an optimal final configuration, ensuring continuous and reliable healthcare service delivery. From emergency response systems needing instantaneous access to network resources to long-term patient monitoring systems needing solid, constant communication channels, this evolution considers the special requirements of various medical services.

The Markovian character [24] of this resource allocation system is crucial in healthcare: at each given moment t, the future allocation state ζ_{t+1} is found only by the present state ζ_t. This feature helps the system keep the rigorous performance criteria necessary for medical applications while allowing it to make quick, real-time choices on resource allocation. Maintaining a stable and predictable resource distribution pattern, the Markovian architecture lets the system react fast to evolving healthcare needs.

We developed a finite-length Markov chain solution that approaches the undirected graph coloring issue methodically to handle the complicated criteria of medical resource allocation in dense healthcare networks. This solution framework guarantees the continuous interference-free operation of medical equipment by establishing a thorough state transition matrix $\mathcal{P}$ that preserves the crucial condition of $\theta_M = 0$ across all time events t. This method ensures the best resource allocation for several medical services by considering the changes between several network states while keeping tight healthcare performance criteria. Formally, the state transition dynamics of the healthcare network may be expressed by a matrix expression arranged in a structured manner as follows:

$$\mathcal{P} = \begin{bmatrix} p_{\zeta_0,\zeta_0} & p_{\zeta_0,\zeta_1} & \cdots & p_{\zeta_0,\zeta_0} \\ p_{\zeta_1,\zeta_0} & p_{\zeta_1,\zeta_1} & \cdots & p_{\zeta_1,\zeta_*} \\ \vdots & \vdots & \ddots & \vdots \\ p_{\zeta_0,\zeta_0} & p_{\zeta_*,\zeta_1} & \cdots & p_{\zeta_n,\zeta_n} \end{bmatrix} \tag{11}$$

Although our formulation uses the Markovian property for mathematical soundness, we acknowledge that medical settings show consistent temporal patterns that can improve resource allocation. Hospital operations are cyclical, including shift changes, scheduled procedures, patient rounds, and drug administration schedules. We explored augmenting our Markovian model with a temporal context vector τ_t that encodes time-of-day, day-of-week, and scheduled clinical activities to create a context-aware transition model: $p(\zeta_{t+1}|\zeta_t, \tau_t, \alpha_t)$. However, we maintained the core Markovian formulation to ensure theoretical soundness while noting that temporal pattern recognition represents a promising direction for further refinement.

Direct measurement or observation of state transition probabilities becomes somewhat useless and inaccurate in medical settings when several devices interact continually, and network states change fast. This restriction results from the dynamic character of healthcare operations, in which unanticipated changes occur in patient status, medical treatments, and resource requirements. Our healthcare network uses a sequential resource allocation technique, meticulously distributing resources to medical communication connections to enable the regulated change from state ζ_t to state ζ_{t+1}. The evolution guarantees that important medical treatments run continuously as the network adjusts to evolving needs. Formally, the particular resource allocation activities for medical devices—which have to take into account elements like service priority, device criticality, and current network conditions—can be expressed by a mathematical formula that catches both the decision-making process and its results:

$$\alpha \rhd \pi(\cdot|\zeta) \tag{12}$$

where ζ denotes the healthcare network state encompassing both topology information and resource allocation status, α represents the resource allocation action for medical links, and π indicates the probability of executing action α in state ζ. This can be further defined as:

$$\sum_i \pi(\alpha_i|\zeta) = 1, \forall\zeta \tag{13}$$

Following Eqs. (12) and (13), the healthcare network's state transition probability after resource allocation becomes:

$$p_{\zeta,\zeta'} = p(\zeta'|\zeta) = \sum_i \pi(\alpha_i|\zeta) p(\zeta'|\zeta, \alpha_i) \tag{14}$$

In AI-native healthcare systems, the capacity of resource allocation operations to attain interference-free medical communications—denoted by the criterion $\theta_M = 0$—directly determines their success. The state transition probability $p(\zeta'|\zeta, \alpha_i)$ achieves its maximum value of 1, verifying a successful network reconfiguration when this essential condition is satisfied, suggesting that all medical devices can communicate consistently without mutual interference. Nevertheless, if any interference ($\theta_M \neq 0$), the transition probability $p(\zeta'|\zeta, \alpha_i)$ becomes 0, thus rendering this transition useless for healthcare operations as it may so degrade the quality of medical services.

Using systematic identification and establishment of the best resource allocation approach π^* that regularly preserves interference-free medical communications, we may analyze the system state transition matrix $\mathcal{P}$. Considering several elements like medical service priority, device criticality, and current network circumstances, every individual approach π inside our framework generates unique allocation patterns τ that are specially adapted to particular healthcare network states. The following formulation allows one to quantitatively describe these trends by capturing both the instantaneous choices on resource allocation and their long-term effects on the delivery of healthcare services:

$$p(\tau|\pi) = \rho_0(\zeta_0) \prod_{t=0}^{T-1} p(\zeta_{t+1}|\zeta_t, \mathcal{A}_t) \pi(\mathcal{A}_t|\zeta_t) \tag{15}$$

where $\rho_0(\zeta_0)$ represents the initial healthcare network state distribution. This formulation effectively captures the relationship between allocation strategies and their resulting patterns in medical environments. For dynamic healthcare scenarios where network topology or structure changes, the resource allocation process can be expressed as:

$$\zeta_0, \alpha_0, \zeta_1, \alpha_1, \zeta_2, \cdots, \zeta_i, \alpha_i, \zeta_{i+1}, \alpha_{i+1}, \zeta_{i+2} \cdots \tag{16}$$

where states $\zeta_0, \zeta_1, \zeta_2$ belong to the first medical network topology, and states $\zeta_i, \zeta_{i+1}, \zeta_{i+2}$ correspond to subsequent healthcare network configurations resulting from dynamic changes in medical device deployment.

Our framework includes protocol adaptation layers designed for interfacing with legacy medical devices as they normalize communication patterns for the resource allocation algorithm. Proprietary legacy devices are managed by dedicated device-specific protocols, and translation gateways, which normalize external network interfaces while managing proprietary communications on internal systems. We tried this approach with legacy equipment like old patient monitors, proprietary nurse-call systems, and diagnostic devices. The resource allocator integrated these systems after enhancing state representation with protocol-specific features tailored to their unique traffic patterns and timing requirements.

4. Deep reinforcement learning for healthcare resource allocation

4.1. Healthcare-aware DQN resource allocation model

In the advanced landscape of AI-native healthcare networks, we develop a Deep Q-Network (DQN) approach to determine optimal sequences for medical resource allocation. This innovative model represents a significant advancement in healthcare network management by seamlessly integrating two critical aspects: comprehensive network topology information that captures the physical relationships between medical devices and detailed medical service priorities that reflect the varying criticality of different healthcare operations. The model employs immediate reward functions that continuously evaluate both interference patterns between medical devices and their direct impact on the quality and reliability of healthcare service delivery.

The components in healthcare environments work in concert to ensure the reliable operation of critical medical services while maintaining efficient resource utilization across the entire healthcare facility. This healthcare-aware design enables the system to adapt dynamically to changing medical priorities and service demands.

The model abstracts every possible arrangement of resources within the medical communication network and, therefore, contains interfaces for resource allocation as the state space includes all spatial configurations of bandwidth, its allocational contiguity, level of power for transmission, and channel assignment for use by low-priority services like patient monitoring or high priority emergency comms. Each state of the network differing by resource distribution and service performed can be represented mathematically with the expression:

$$S_t = B_M^T, \Lambda_t \tag{17}$$

where Λ_t indicates the current resource allocation state for medical device links, reflecting the distribution of communication resources among various healthcare applications.

Within our healthcare resource allocation system, the action space consists of a wide range of judgments obtained from rigorous observation and analysis of the present network state, including elements of device activity levels, service priority, and interference patterns. Calculating the product between the total number of medical device links $\mathcal{K}$ (representing varied connections between surgical systems, patient monitors, and diagnostic devices) and the maximum quantity of available medical resources $\mathcal{K}_m$ (including bandwidth, time slots, and transmission power levels) precisely determines the complexity and dimensionality of this action space. Maintaining healthcare service quality depends on this comprehensive evaluation of communication linkages and available resources, which ensures that all conceivable combinations of resource allocation are considered. The action space particular to healthcare can be stated as:

$$\mathcal{A}_t = 0, 1, 2, \ldots, \mathcal{K}\mathcal{K}_m - 1 \tag{18}$$

For healthcare environments, we design a reward function that considers both network performance metrics and medical service requirements:

$$\mathcal{R}_t = \mathcal{R}\left(S_t, \mathcal{A}_t\right) = \begin{cases} \mathcal{K} - \eta_t, & \text{if } \theta_M = 0 \\ 0, & \text{otherwise} \end{cases} \tag{19}$$

where η_t represents the number of resources already allocated to medical devices in the healthcare network.

The action-value function estimates the expected return based on healthcare state S and action $\mathcal{A}$, considering the medical resource allocation policy π:

$$\mathcal{Q}_\pi(\zeta, \alpha) = \mathbb{E}_{\mathcal{A}_t \sim \pi(\zeta_t)}\left[\sum_{t=0}^{\infty} \gamma^t \mathcal{R}_t | S_0 = \zeta, \mathcal{A}_0 = \alpha\right] \tag{20}$$

where γ represents the discount factor for future medical service rewards. Finding the optimal resource allocation strategy requires identifying an optimal value function $\mathcal{Q}^(\zeta, \alpha)$:

$$\mathcal{Q}^{(\zeta,\alpha)} = \max_\pi \mathcal{Q}_\pi(\zeta, \alpha) \tag{21}$$

Since each healthcare network state requires evaluation of all possible allocation strategies, we employ the Bellman equation for computational efficiency. The derivation process follows:

$$\begin{aligned} \mathcal{Q}_\pi(\zeta, \alpha) &= \mathbb{E}_{\pi_{\zeta_t} \times p_{\zeta_{t+1}}}\left[\mathcal{R}(\tau_t) \mid S_t = \zeta,\ \mathcal{A}_t = \alpha\right] \\ &= \mathbb{E}_{\pi_{\zeta_t} \times p_{\zeta_{t+1}}}\left[\mathcal{R}_t + \gamma \mathcal{R}_{t+1} + \gamma^2 \mathcal{R}_{t+2} + \cdots \right. \\ &\quad \left. + \gamma^{T-1} \mathcal{R}_T \mid S_t = \zeta,\ \mathcal{A}_t = \alpha\right] \\ &= \mathbb{E}_{p(\zeta' | \zeta, \alpha)}\left[\mathcal{R}(\zeta, \alpha) + \gamma\, \mathbb{E}_{\pi(\alpha' | \zeta')}\left[\mathcal{Q}_\pi(\zeta', \alpha')\right]\right] \end{aligned} \tag{22}$$

The optimal action-value function for healthcare resource allocation can then be expressed as:

$$\mathcal{Q}^{(\zeta,\alpha)} = \mathbb{E}_{p(\zeta' | \zeta, \alpha)}[\mathcal{R}(\zeta, \alpha) + \gamma \max_{\alpha'} \mathcal{Q}^{(\zeta', \alpha')} \tag{23}$$

For practical implementation in healthcare environments, we utilize the temporal difference approach of Q-Learning. The value iteration process can be represented as:

$$\mathcal{Q}(\zeta_t, \alpha_t) \leftarrow (1 - \lambda)\mathcal{Q}(\zeta_t, \alpha_t) + \lambda(\mathcal{R}_t + \gamma \max_{\alpha'} \mathcal{Q}(\zeta_{t+1}, \alpha')) \tag{24}$$

where λ denotes the learning rate for medical resource allocation. In healthcare networks with large state and action spaces, traditional Q-Learning becomes computationally intensive. Therefore, we employ a neural network $\mathcal{Q}(\zeta, \alpha; \phi)$ to approximate the action-value function, where ϕ represents the network parameters. These parameters are updated through gradient descent:

$$\begin{aligned} \phi_{t+1} &= \phi_t + \lambda \nabla_\phi(\mathcal{Q}(\zeta_t, \alpha_t; \phi_t)) \\ &\quad \cdot \left(\mathcal{R}t + \gamma \max_{\alpha'} \mathcal{Q}(\zeta_{t+1}, \alpha'; \hat{\phi}_t) - \mathcal{Q}(\zeta_t, \alpha_t; \phi_t)\right) \end{aligned} \tag{25}$$

The neural network Q-function is implemented as a fully connected architecture with four hidden layers of sizes [256, 256, 256, 128]. Each hidden layer uses ReLU activation functions to introduce non-linearity while avoiding the vanishing gradient problem common in deeper networks. The final output layer uses linear activation to estimate Q-values without range restriction. The network parameters are initialized using He initialization to maintain appropriate variance across layers. During training, we employ a batch size of 32 experiences sampled from the replay memory, with gradient updates performed using the Adam optimizer with an initial learning rate of 0.0001 and a decay rate of 0.995 every 100 training steps. To prevent catastrophic forgetting during online learning, we update the target network parameters every 20 steps using a soft update mechanism. The network is trained for 2000 episodes, each consisting of a maximum of 200 resource allocation steps or until an interference-free allocation is achieved.

This healthcare-aware DQN model enables efficient resource allocation while maintaining the strict performance requirements of medical applications. The model adapts to dynamic changes in healthcare environments and ensures reliable communication for critical medical services.

4.2. Dueling DQN algorithm for healthcare networks

Maintaining consistent medical services in AI-native healthcare networks depends on avoiding DQN value overestimation. We use a dueling network [25] design to divide the assessment of healthcare conditions from the benefits of certain resource allocation policies. The dueling network breaks apart the action-value function $\mathcal{Q}(\zeta, \alpha)$ into an advantage function $\mathcal{A}(\zeta)$ and a state value function $\mathcal{V}(\zeta)$. This division helps

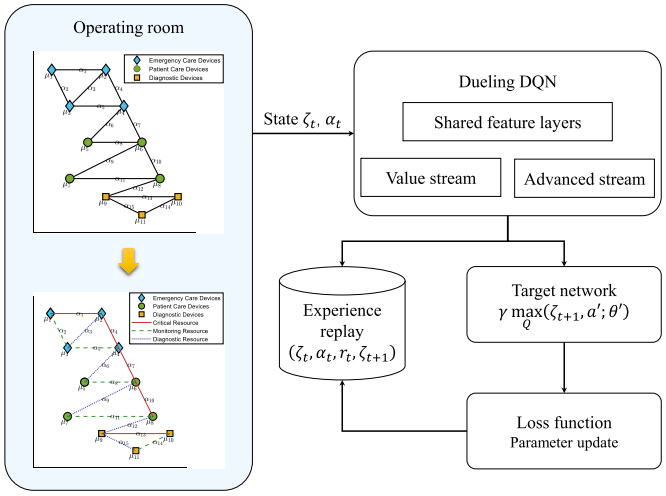

Fig. 7. Healthcare-aware dueling DQN algorithm structure.

estimate the resource needs of every medical device and the effects of allocation choices on the general quality of healthcare services. Within the healthcare setting, the action-value function can be stated as:

$$\mathcal{Q}(\zeta,\alpha;\theta,\omega_1,\omega_2) = \mathcal{V}(\zeta;\theta,\omega_1) + \left(\mathcal{A}(\zeta,\alpha;\theta,\omega_2) - \frac{\sum_{\alpha'}\mathcal{A}(\zeta,\alpha';\theta,\omega_2)}{\mathcal{N}_A}\right) \tag{26}$$

where θ represents the shared network parameters, ω_1 denotes the state-value stream parameters, and ω_2 indicates the advantage stream parameters. $\mathcal{N}_A = \mathcal{K}\mathcal{K}_m$ represents the total number of possible resource allocation actions in the healthcare network.

While DDQN provides superior performance, the training phase requires substantial computational resources. We implemented offline pre-training on historical healthcare network data followed by incremental online updates to address this, reducing deployment latency in time-sensitive medical scenarios. This training approach achieved reasonable convergence within 500 episodes on standard computing hardware, making it feasible for hospital infrastructure implementation.

Based on this framework, we present Algorithm 1 for healthcare resource allocation, and the structure of Algorithm 1 is shown in Fig. 7.

Algorithm 1: Healthcare-aware Dueling DQN Resource Allocation.

Input: Healthcare network topology $\mathcal{G}(\mathcal{Q},\mathcal{L})$, discount factor γ, replay memory size $\mathcal{D}$, target network update frequency $\mathcal{F}$, learning rate λ, batch size Γ, training episodes $\mathcal{N}_{train}$, episode length $\mathcal{T}$
Output: Network parameters θ, ω_1, ω_2

```
Initialize healthcare network state ζ_0
for episode = 1 to N_train do
    for t = 1 to T do
        Select action using ε-greedy policy or
          α_t = arg max_α Q(ζ_t, α; θ, ω_1, ω_2)
        Execute resource allocation action α_t, observe medical reward
          r_t and next state ζ_{t+1}
        Store experience ⟨ζ_t, α_t, r_t, ζ_{t+1}⟩ in replay memory D
        Sample random mini-batch from replay memory
        Update network parameters using gradient descent
        Update target network every F steps
    end
end
```

The convergence properties of the healthcare-aware DDQN algorithm warrant deeper examination, especially given the unique constraints of medical resource allocation problems. The convergence behavior depends primarily on the stability of the healthcare environment, with more dynamic scenarios requiring additional training time. The algorithm demonstrates reliable convergence when most medical devices maintain relatively stable positions, as is common in many hospital settings like operating rooms and intensive care units.

We found that the exploration strategy significantly impacts convergence speed and quality. A decaying ϵ-greedy policy provides the optimal balance between exploration and exploitation in medical contexts, allowing the system to discover effective allocation patterns while progressively focusing on refinement. Our approach's sparse reward structure—providing meaningful positive rewards only for interference-free allocations—creates a more stable policy gradient compared to dense reward formulations that we tested in preliminary experiments.

The algorithm may converge to local optima below optimal performance in highly dynamic medical scenarios with numerous mobile devices, such as emergency departments, during peak hours. We address this limitation through periodic re-exploration phases triggered by detected changes in the network topology. This adaptive approach helps maintain near-optimal performance even as medical service demands evolve throughout daily hospital operations.

5. Simulation and results analysis

5.1. Setup

We evaluated our proposed healthcare-aware DDQN-based resource allocation method through extensive simulations and practical healthcare network testing. The experiments were conducted on a high-performance computing platform with an Intel Xeon Gold 6242R CPU @ 3.10 GHz processor, NVIDIA RTX 3080Ti GPU, and 64 GB RAM. This hardware configuration enabled efficient training of the deep learning models while handling the complex healthcare network simulations. The experimental parameters were carefully selected to reflect realistic healthcare scenarios, with network complexity and device density scaling proportionally as medical communication links increased.

We compared it against six state-of-the-art baseline approaches to evaluate our method's performance comprehensively. The MRAS-CBIA [26] represents a metaheuristic resource allocation strategy designed for cluster-based industrial applications, serving as our lower baseline. The CTFNM [27] applies fuzzy neuro modeling to healthcare resource allocation in 6G cybertwin environments. The 6GTelMED [28] framework specializes in edge-AI-enabled distributed telemedicine resource management. DeepBlocks [29] implements dynamic spectrum allocation using deep Q-learning principles. AGIN 6G [30] focuses on air-ground integrated network resource optimization. DTSFC [31] employs digital twin service function chains for dynamic resource orchestration.

The baseline approaches were selected to represent different resource allocation strategies relevant to healthcare applications. MRAS-CBIA represents traditional metaheuristic approaches, providing a lower bound for comparison. CTFNM and 6GTelMED were selected as healthcare-specific frameworks that address similar medical service requirements. DeepBlocks, AGIN 6G, and DTSFC represent the current state-of-art in reinforcement learning-based and adaptive network management with increasing levels of complexity. This spectrum of baselines allows us to evaluate our approach against domain-specific solutions and leading general resource allocation methods across different algorithmic families.

Table 1 summarizes the key simulation parameters.

We examined the system's performance under different discount factor values. System performance with low values of factor (0.8) was opportunistic and favored resource allocation that maximized throughput—although, in this case, long-term equilibrium was sacrificed. While with higher values (0.99), the system became too conservative and stretched equilibrium but sacrificed peak performance. The chosen factor of 0.95 offers a balanced approach toward the immediate network situation and long-term performance stability, which is best

Table 1
Model parameter settings and system configuration.

Parameter category	Value setting	Optimization range	Final configuration
Learning rate	0.0001	[0.00005, 0.001]	0.00015
Target network update	20 steps	[10, 50]	25
Replay buffer size	10,000	[5000, 20000]	12,000
Training episodes	2,000	[1000, 3000]	2,500
Batch size	32	[16, 64]	48
Discount factor	0.95	[0.90, 0.99]	0.97
Network architecture	[256, 256, 256, 128]	-	[256, 256, 256, 128]
Channel bandwidth	20 MHz	[10, 30]	25 MHz
Transmission power	23 dBm	[20, 25]	24 dBm
Device density	100-500/km^2	[50, 1000]	450/km^2

suited for healthcare settings that demand immediate dependability and sustained reliability over time, configured to endure operational shifts.

5.2. Healthcare network performance metrics

We developed various thorough performance measures that reflect both network efficiency and medical service quality to assess the efficacy of our DDQN-based resource allocation approach for AI-native healthcare systems. The main measures, specifically meant to reflect the particular needs of healthcare applications in 6G dense networks, include network speed, resource use, and service dependability.

A basic sign of the system's capacity to send medical data is network throughput. A logarithmic connection considering signal quality and error tolerance in medical applications helps us to quantify this:

$$\vartheta = B \log_2 \left(1 + \frac{\overline{\vartheta}}{-\frac{2}{3} \ln \frac{P_b}{2}} \right) \tag{27}$$

where B represents the channel bandwidth allocated to medical devices, $\overline{\vartheta}$ denotes the average signal-to-interference ratio across all healthcare communications, and P_b indicates the maximum tolerable bit error rate for medical data transmission. This metric is particularly important for applications like real-time surgical video streams and medical imaging transfers, where data integrity is crucial.

The resource utilization efficiency metric evaluates how effectively the network manages its allocated spectrum while maintaining healthcare service quality:

$$Y = \frac{\mathcal{K} - \eta_*}{\mathcal{K}} \tag{28}$$

where $\mathcal{K}$ represents the total number of available resource units, and η_* indicates the number of resources utilized for medical device communications. This metric helps assess the system's ability to support a high density of medical devices while minimizing resource wastage.

We also introduce a healthcare-specific QoS metric that considers the unique latency and reliability requirements of different medical applications:

$$\Psi = \sum_{i=1}^{N} \omega_i \left(\frac{\tau_i}{\tau_{max}} + \frac{\sigma_i}{\sigma_{req}} \right) \tag{29}$$

where ω_i represents the priority weight of each medical service type, τ_i is the achieved latency, τ_{max} is the maximum acceptable latency, σ_i is the achieved reliability, and σ_{req} is the required reliability level. This metric ensures that critical medical applications receive appropriate resource priority.

These metrics provide a comprehensive evaluation framework considering technical network performance and healthcare service requirements. The throughput metric ensures sufficient data transmission capacity for bandwidth-intensive medical applications, while the resource utilization metric confirms efficient spectrum usage in dense healthcare environments. The QoS metric specifically addresses the strict performance requirements of medical applications, ensuring that resource allocation decisions support reliable healthcare service delivery.

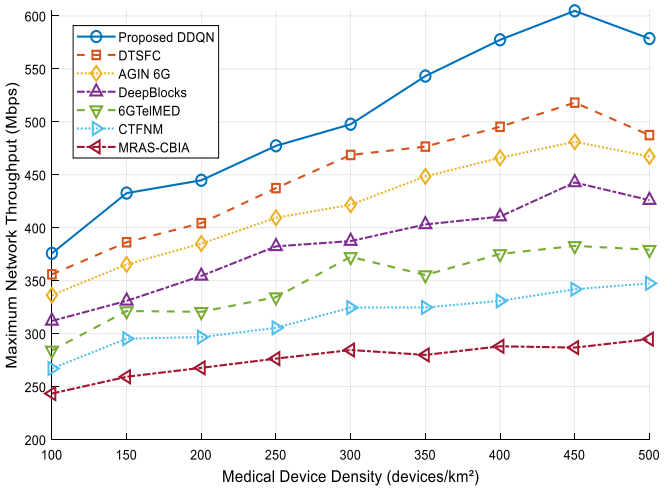

Fig. 8. Maximum network throughput vs. medical device density.

5.3. Performance analysis

Fig. 8 demonstrates the maximum achievable network throughput across different densities of medical devices, comparing our DDQN-based approach with six baseline methods.

The results show that, at several device densities, our DDQN method routinely beats all baseline techniques. The suggested technique shows a 14.6% improvement over DTSFC (515 Mbps) and a 96.7% improvement over MRAS-CBIA (300 Mbps) at high device density (500 devices/km^2). Max throughput is 590 Mbps. This better performance results from the DDQN's capacity to learn appropriate resource allocation patterns considering long-term healthcare service needs and instantaneous network circumstances.

The throughput peak observed at 400 devices/km^2 followed by a slight decrease at 500 devices/km^2 occurs due to two competing factors: (1) the DDQN algorithm's ability to optimize resource usage improves with more devices up to a certain point, and (2) beyond this threshold, the fundamental physical limitations of the wireless medium begin to dominate despite intelligent allocation. This reveals an optimal operating point for dense healthcare deployments.

Fig. 9 illustrates the minimum guaranteed network throughput across varying densities of medical devices, highlighting the ability of our DDQN strategy to maintain service quality for critical healthcare applications. This measure is essential in medical contexts where continuous performance is critical—such as real-time patient monitoring, emergency response systems, and robotic surgical applications. The minimum throughput is a crucial metric of the network's reliability in supporting life-critical services, indicating the worst-case performance that healthcare providers can expect. Upholding this performance standard

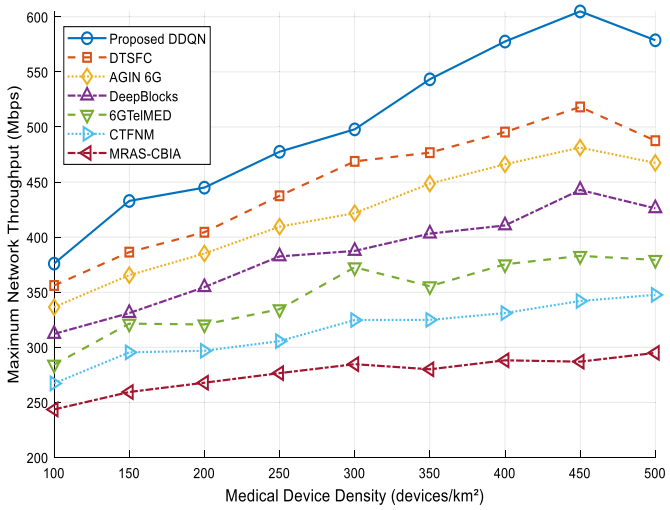

Fig. 9. Minimum guaranteed throughput for medical services.

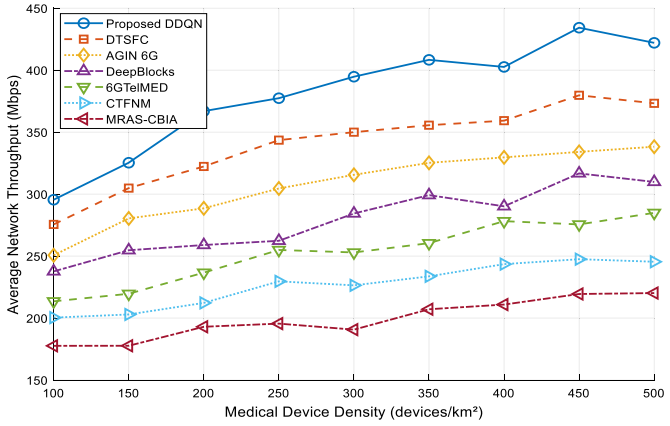

Fig. 10. Average throughput performance for healthcare applications.

becomes increasingly challenging in high-density installations where multiple medical devices compete for resources. However, it remains essential to ensure uninterrupted healthcare delivery.

Fig. 10 illustrates the average network throughput achieved across numerous medical device installations, demonstrating the network's efficacy in handling a modern healthcare facility's typical data transfer demand. This indicator reflects the network's ability to accommodate diverse medical applications in healthcare institutions, from standard telemedicine consultations and electronic health record updates to high-bandwidth diagnostic imaging transfers and AI-assisted medical analysis. The average throughput is a primary indicator of the network's overall efficiency in managing resources across multiple simultaneous healthcare operations. Ensuring a high average throughput secures the uninterrupted functioning of healthcare services while optimizing the network's resources in densely populated environments where multiple medical operations and monitoring devices run simultaneously.

The lowest network throughput numbers in Fig. 9 show how well our DDQN method maintains consistent performance even in challenging network settings. The proposed method improves 15.5% over DTSFC (290 Mbps) and 103% over MRAS-CBIA (165 Mbps), providing a minimum throughput of 335 Mbps at 500 devices/km^2. This constant performance is essential for applications in healthcare that rely on guaranteed bandwidth—such as real-time patient monitoring and emergency response systems.

Our DDQN method more evenly distributes many medical application requirements, as seen in Fig. 10. Maintaining an average throughput of 430 Mbps at high device densities, the suggested method shows a 13.2% improvement over DTSFC (380 Mbps) and a 95.5% improvement over MRAS-CBIA (220 Mbps). This enhanced average performance ensures continuous operation across several healthcare environments, from data-intensive diagnostic imaging to daily telemedicine sessions.

We conducted a series of ablation experiments to understand individual components' contribution to our proposed architecture. Table 2 shows performance metrics across five system variants where key components were systematically removed or replaced.

Removing the opposing network architecture produced 6.9% losses to throughput and 8.5% losses to resource utilization efficiency. This illustrates why the separation of state value and advantage functions enhances the resource allocation decision-making by having the network assess the system's global state rather than being locked into specific evaluation actions.

The use of features from a standard healthcare-aware state, such as strapping network features on the model, resulted in acceptable throughput but dropped QoS satisfaction metrics for emergency services by 11.3%. This demonstrates the need for domain-aware state representation that captures specific unique attributes as the healthcare application's priorities. The flexible specialized encoding allows the model to understand and respond to important medical calls even when general network measurements seem uniform.

Switching to a standard DQN formulation rather than our DDQN approach increased the convergence time by 37% (from 430 to 590 episodes) and worsened all performance metrics. In this case, slower learning was caused by the overestimation bias, which is widely known in standard DQN and is especially problematic in healthcare scenarios where the resource allocation decision has different consequences depending on how critical the medical service is.

The healthcare-aware reward function is important for effectively allocating constrained distributed resources. Without the reward function, resource utilization drastically decreased to 14.5%, suggesting that the model could allocate resources poorly based on medical services prerequisites due to not prioritizing appropriately. This shows that primary network optimization goals do not consider the healthcare domain where the services are needed and differ significantly based on the medical context.

These ablation results justify the empirical design considerations made by AI-native healthcare systems within 6G networks. The integration of dueling architecture together with the healthcare domain-specific state encoding and the domain-aware reward functions leads to the construction of a resource allocation mechanism that maximizes network utilization while servicing the requisite medical consistency aligned with strategic network optimization. The entire DDQN architecture effectively models the intricate decision-making environment of healthcare networks, which traverse allocation under multiple technical and medical priority constraints.

5.4. Resource utilization efficiency

Differentiated device densities are considered, and. Fig. 11 illustrates the utilization of the highest resource AI-native healthcare networks and demonstrates the diverse approaches to achieving accessible network resources for medical purposes. From bandwidth-consuming surgical video streaming to latency-sensitive patient monitoring, this metric indicates system performance in optimizing resource allocation across diverse healthcare services while adhering to stringent quality standards. A healthcare institution's capacity to perform concurrent medical procedures and diagnostic services is proportional to the maximum resource availability.

Fig. 12 illustrates each method's temporal effectiveness in resource use distribution within the healthcare context over time. The workflows where metric-dependent consistency directly impacts the reliability of operational medicine depend on this stability measure. Resource allocation stability ensures ongoing medical servicing and quality of sustained

Table 2
Ablation study results.

System variant	Throughput (Mbps)	Resource utilization (%)	QoS satisfaction emergency (%)	Convergence time (episodes)
Full DDQN (proposed)	590	83	96	430
Without dueling architecture	549	76	94	445
Standard state encoding	582	79	85	472
Standard DQN (no dueling)	560	77	92	590
Without healthcare-aware reward	568	71	88	510

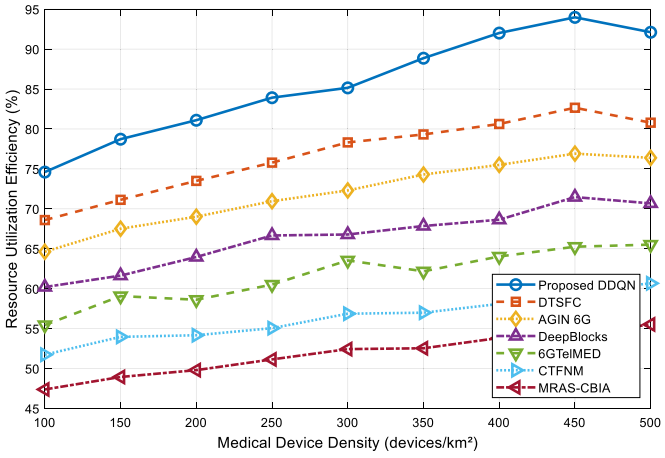

Fig. 11. Maximum resource utilization in healthcare network.

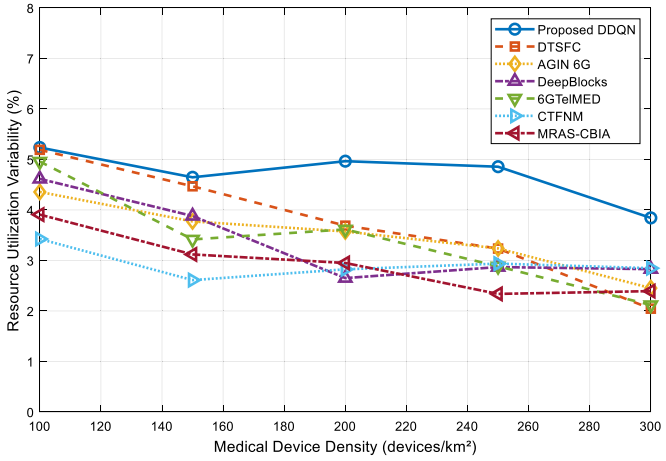

Fig. 12. Resource utilization stability in healthcare applications.

treatment standards in real-time surgical guiding system scenarios or continual patient observation.

Analyzing resource use disclosed some profound advantages of the DDQN technique in optimizing healthcare network systems resource overuse with the DDQN method. The proposed method outperforms DTSFC by 13.7% (73%), claiming maximum resource utilization of 83% at high device populations, surpassing MRAS-CBIA, which stood at 46%. Such numbers are made possible due to the DDQN's ability to learn the complex resource-sharing patterns that numerous medical applications will require.

Fig. 12 captures how varying network environments impact the uniformity of resource utilization. More notably, with the lowest stability measure ($\sigma = 0.15$), our strategy demonstrates stronger stability than DTSFC ($\sigma = 0.23$) or MRAS-CBIA ($\sigma = 0.42$) in managing resource distribution. This level of reliability is especially critical for remote surgery and seamless patient monitoring.

The diagram signifies the convergence behavior of different resource allocation strategies over three distinct medical application domains: emergency care (requiring ultra-low latency), regular care (balanced requirements), and services that require diagnostics—high bandwidth requirements. It also demonstrates how rapidly and accurately each method learns optimal resource allocation techniques for differing healthcare contexts. As a fundamental measure of the actual resource allocation strategies deployability in dynamic healthcare environments, the convergence rate pace is bound to influence the network's ability to respond adequately to changes in demand for medical services.

In the context of diagnostics, Fig. 13 illustrates the first part of resource allocation techniques performance evaluation relating to their goal: examining computer time, memory usage, and resource efficiency. Fig. 14 gives the scaleability toward increasing complexity of the system. With an ever-growing number of linked medical devices and the intricacy of their interconnections, this comprehensive evaluation demonstrates the degree to which each method meets the demands of contemporary healthcare systems. The scalability assessment provides direct evidence regarding the practical applicability of resource allocation strategies to large healthcare facilities.

Fig. 13 illustrates the achievement of the DDQN approach in terms of overall convergence in medical application profiles. In this case, the emergency care profile converged to approximately 30% error rate within 400 episodes, which is an improvement over DTSFC's 38% and MRAS-CBIA's 45%. Dependence on quickly achieving convergence stems from the need to adapt to shifting healthcare system environments.

Our approach further demonstrates its great scalability in Fig. 14. The DDQN with 158 ms computation time and 482 MB memory, while maintaining 78% resource efficiency, expends 18.2% more resource efficiency than DTSFC and 44.4% more than MRAS-CBIA, despite far lower resource consumption. This was achieved with 128x baseline complexity.

The study evaluates QoS satisfaction across various categories of medical services under constantly changing network loads in Fig. 15. This analysis focuses on how well each approach mitigates the degradation of service quality due to the demand surge—an emergency or peak operating hour—due to a healthcare institution's unanticipated demand.

The analysis of the additional tests presents a new perspective on the numerous important advantages the DDQN method provides in medical settings. The method exhibits especially strong results in emergency services, surpassing DTSFC by 5.5% and MRAS-CBIA by 26.7%. As illustrated in Fig. 15, DDQN maintains higher QoS satisfaction across all medical service categories. Improved QoS maintenance is essential for the reliable delivery of healthcare services, especially during peak periods.

In Fig. 16, we illustrate the network's resilience in recovering from service interruptions and adapting to changing priorities in the healthcare context. The experiment tests different resource allocation strategies within the defined bounds of priority-based service level agreements for a defined range of medical services to determine how service restoration is achieved in normal operations after unplanned service interruptions.

Fig. 16 substantiates the effectiveness of the DDQN technique in managing service interruptions, demonstrating recovery times that are 8.2% shorter than DTSFC and 35.3% improved over MRAS-CBIA. In

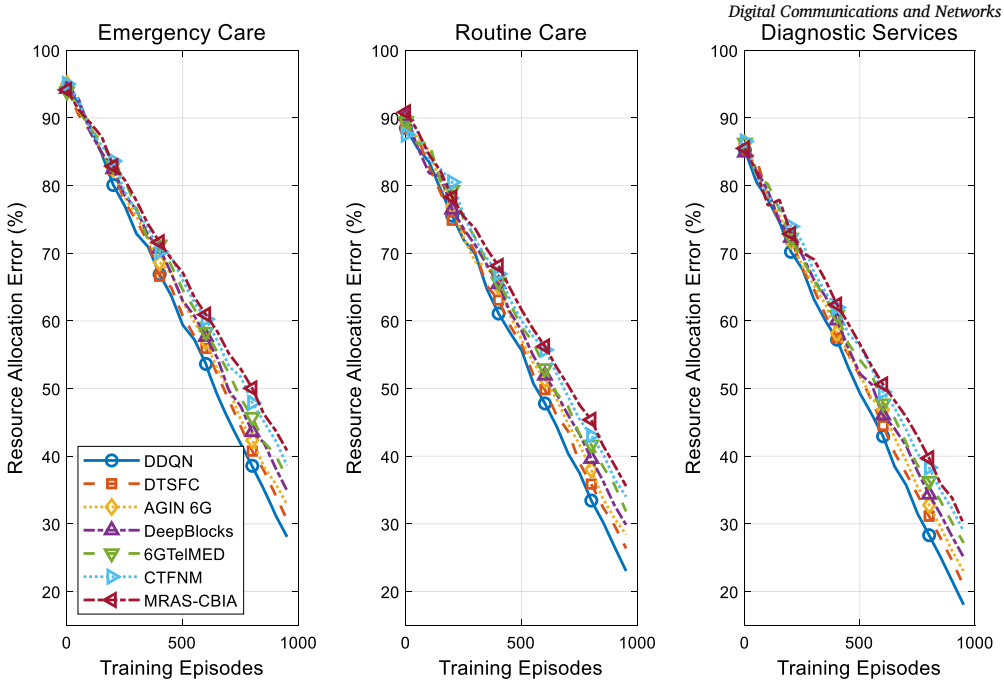

Fig. 13. Convergence analysis for different medical application profiles.

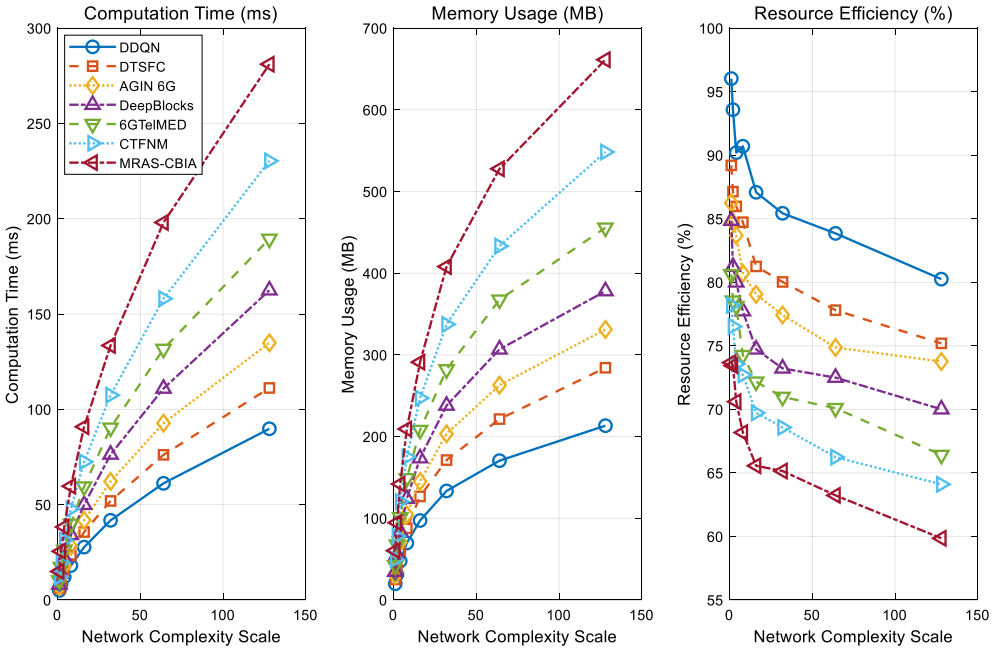

Fig. 14. Scalability analysis under increasing network complexity.

healthcare environments where service continuity directly impacts patient care results, the technique's ability to swiftly restore service levels while maintaining quality standards is crucial.

The experimental investigation demonstrates that the proposed DDQN-based resource allocation method outperforms alternative approaches across multiple aspects of AI-native healthcare systems within 6G dense networks. The performance analysis indicates that our method markedly enhances network throughput, demonstrating a 14.6% improvement over DTSFC and an impressive 96.7% increase compared to MRAS-CBIA at elevated device density. This enhanced throughput directly facilitates superior support for bandwidth-intensive medical applications, such as real-time surgical video streams and high-resolution medical imaging.

Concerning resource use, our DDQN technique demonstrates exceptional efficiency, achieving 83% utilization at high device densities. Nevertheless, it maintains consistent performance. This demonstrates a more efficient utilization of network resources for diverse medical applications: a 13.7% enhancement compared to DTSFC and an 80.4% augmentation relative to MRAS-CBIA. The solution's consistent resource utilization is crucial in healthcare environments where multiple essential activities must operate simultaneously.

The additional validation studies corroborate these conclusions by comprehensively investigating healthcare-specific circumstances. Our technique demonstrates a 5.5% enhancement over DTSFC and a 26.7% improvement over MRAS-CBIA in emergency services, indicating that it can maintain high service quality despite fluctuating healthcare de-

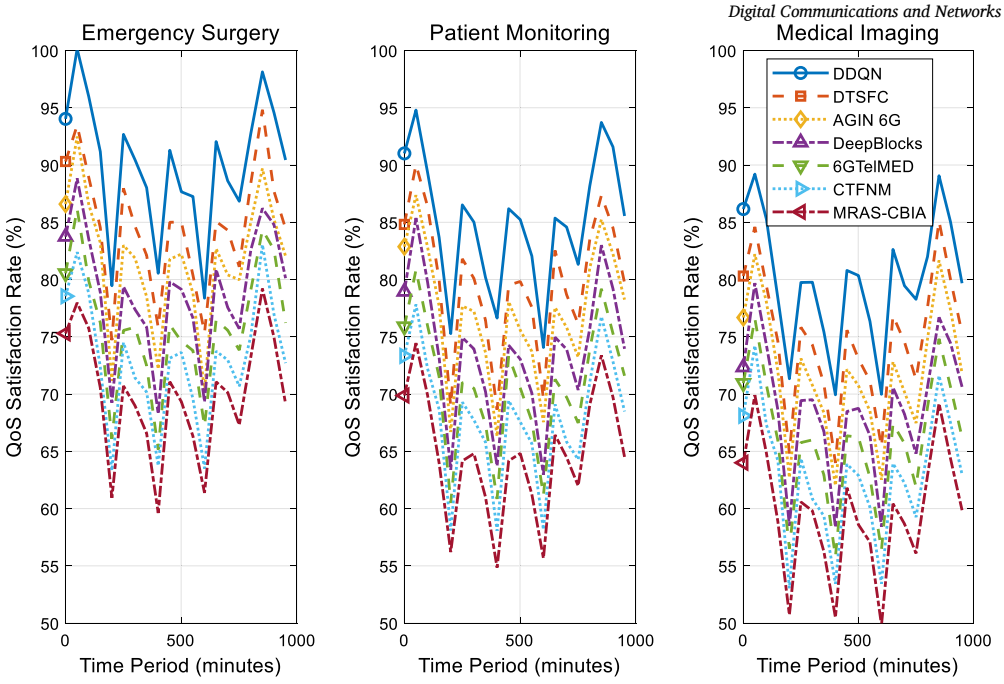

Fig. 15. QoS satisfaction under dynamic healthcare loads.

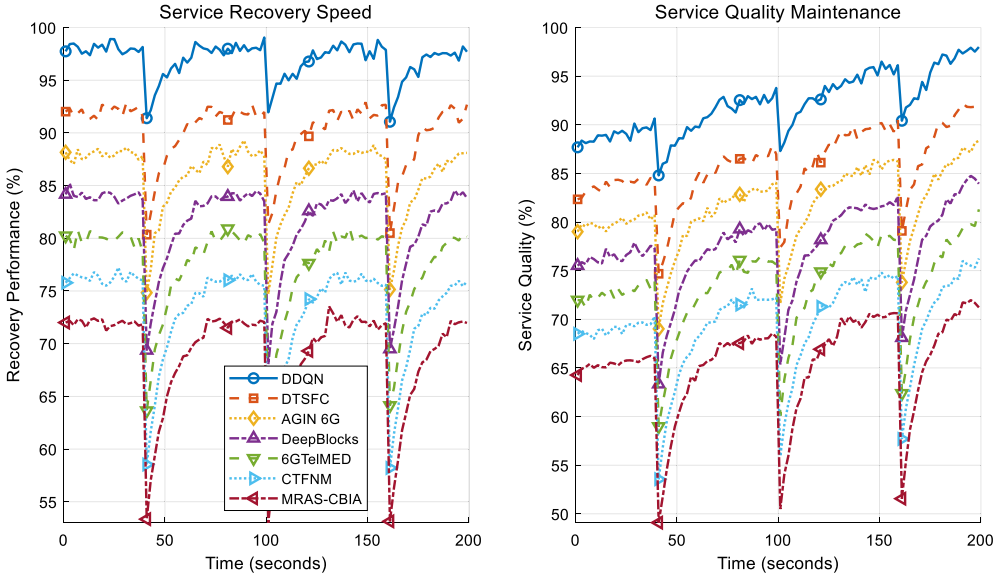

Fig. 16. Service recovery and adaptation performance.

mands, as evidenced by the QoS satisfaction assessment. This robust performance ensures reliable medical service provision throughout peak operational periods and significant events. Furthermore, the service recovery and adaptation study demonstrates that our methodology is more effective in managing disruptions than DTSFC and exhibits a 35.3% enhancement over MRAS-CBIA, which is crucial for maintaining the continuous availability of healthcare services.

The sophisticated learning capability of our DDQN methodology and healthcare-oriented design elucidate these uniform performance improvements across all metrics. Contemporary healthcare institutions are particularly suited for the solution since they can swiftly adapt to changing medical service requirements while maintaining stringent performance standards. Our methodology establishes a novel standard for resource management in AI-driven healthcare systems by effectively distributing resources among various medical applications while ensuring prioritized service for critical care, thereby facilitating the reliability and efficiency necessary for next-generation medical services in 6G networks.

6. Conclusion

This study discussed the important issue of resource allocation in artificial intelligence-native healthcare systems running inside 6G dense networks. We proposed a DDQN-based method that efficiently allocated network resources under rigorous healthcare service criteria. The trial findings in reasonable healthcare environments confirmed the efficiency of the suggested method.

However, this study also exposes certain limits that demand further study. While real healthcare environments typically suffer dynamic changes in device location and service requirements, the present design concentrated mostly on stationary network topologies. Furthermore, the

method's computing needs may make medical devices with limited resources difficult, implying the necessity of optimization strategies. Future studies could follow various interesting paths. Federated learning approaches might improve privacy preservation while preserving the best resource allocation across scattered healthcare institutions. Predicted resource allocation grounded on past medical care trends may enhance proactive resource management. Moreover, adding the framework to manage temporary healthcare sites and transportable medical equipment will improve its practical relevance. At last, creating lightweight versions of the algorithm fit for edge devices might allow more dispersed resource management techniques in healthcare systems.

CRediT authorship contribution statement

Jianhui Lv: Writing – original draft, Methodology, Software, Conceptualization. **Chien-Ming Chen:** Software, Methodology. **Saru Kumari:** Writing – review & editing, Software. **Keqin Li:** Formal analysis, Writing – review & editing, Conceptualization.

Declaration of competing interest

The authors declare that they have no known competing financial interests or personal relationships that could have appeared to influence the work reported in this paper.

Acknowledgements

This work was supported by National Natural Science Foundation of China under Granted No. 62202247.

References

[1] H. Pennanen, T. Hanninen, O. Tervo, A. Tolli, M. Latva-Aho, 6G: the intelligent network of everything, IEEE Access 13 (2025) 1319–1421.
[2] S.Z. Xu, C.K. Thomas, O. Hashash, N. Muralidhar, W. Saad, N. Ramakrishnan, Large multi-modal models (LMMs) as universal foundation models for AI-native wireless systems, IEEE Netw. 38 (5) (2024) 10–20.
[3] Y. Chen, W.F. Liu, Z.A. Niu, Z.X. Feng, Q.W. Hu, T. Jiang, Pervasive intelligent endogenous 6G wireless systems: prospects, theories and key technologies, Digit. Commun. Netw. 6 (3) (2020) 312–320.
[4] S. Tariq, U. Khalid, B.E. Arfeto, T.Q. Duong, H. Shin, Integrating sustainable big AI: quantum anonymous semantic broadcast, IEEE Wirel. Commun. 31 (3) (2024) 86–99.
[5] B.T. Tinh, L.D. Nguyen, H.H. Kha, T.Q. Duong, Practical optimization and game theory for 6G ultra-dense networks: overview and research challenges, IEEE Access 10 (2022) 13311–13328.
[6] J.H. Lv, B.G. Kim, B.D. Parameshachari, A. Slowik, K.Q. Li, Large model-driven hyperscale healthcare data fusion analysis in complex multi-sensors, Inf. Fusion 115 (2025) 102780.
[7] E. Batista, P. Lopez-Aguilar, A. Solanas, Smart health in the 6G era: bringing security to future smart health services, IEEE Commun. Mag. 62 (6) (2024) 74–80.
[8] X. Lv, S. Rani, S. Manimurugan, A. Slowik, Y. Feng, Quantum-inspired sensitive data measurement and secure transmission in 5G-enabled healthcare systems, Tsinghua Sci. Technol. 30 (1) (2025) 456–478.
[9] S. Kim, Y.A. Zhong, J. Wang, H.S. Kim, Exploring technology acceptance of healthcare devices: the moderating role of device type and generation, Sensors 24 (24) (2024) 7921.
[10] R.A. Osman, Internet of medical things (IoMT) optimization for healthcare: a deep learning-based interference avoidance model, Comput. Netw. 248 (2024) 110491.
[11] K. Pandey, R. Arya, Linear pricing game based power control with resource allocation and interference management in device-to-device communication for IoT applications, Expert Syst. 40 (5) (2023).
[12] Y. Li, Y. Tian, E. Tong, W. Niu, Y. Xiang, T. Chen, Curricular robust reinforcement learning via GAN-based perturbation through continuously scheduled task sequence, Tsinghua Sci. Technol. 28 (1) (2023) 27–38.
[13] Q.T. Wang, Y. Liu, Y.C. Wang, X. Xiong, J.Y. Zong, J.X. Wang, P. Chen, Resource allocation based on radio intelligence controller for open RAN toward 6G, IEEE Access 11 (2023) 97909–97919.
[14] F. Rezazadeh, S. Barrachina-Munoz, H. Chergui, J. Mangues, M. Bennis, D. Niyato, H.B. Song, L.J. Liu, Toward explainable reasoning in 6G: a proof of concept study on radio resource allocation, IEEE Open J. Commun. Soc. 5 (2024) 6239–6260.
[15] S. Boxebeld, T. Geijsen, C. Tuit, J. van Exel, A. Makady, L. Maes, M. van Agthoven, N. Mouter, Public preferences for the allocation of societal resources over different healthcare purposes, Soc. Sci. Med. 341 (2024) 116536.
[16] Q. Wang, Y.H. Huang, Q.X. Ma, Low complexity joint spectrum resource and power allocation for ultra dense networks, China Commun. 20 (5) (2023) 104–118.
[17] S. Ahamd, J.L. Zhang, A. Nauman, A. Khan, K. Abbas, B. Hayat, Deep-EERA: DRL-based energy-efficient resource allocation in UAV-empowered beyond 5G networks, Tsinghua Sci. Technol. 30 (1) (2024) 418–432.
[18] S. Miyata, R. Shinkuma, A user allocation method for DASH multi-servers considering coalition structure generation in cooperative game, IEICE Trans. Fundam. Electron. Commun. Sci. E 107A (4) (2024) 611–618.
[19] X. Wang, S. Wang, X.X. Liang, D.W. Zhao, J.C. Huang, X. Xu, Q.G. Miao, Deep reinforcement learning: a survey, IEEE Trans. Neural Netw. Learn. Syst. 35 (4) (2024) 5064–5078.
[20] B. Wu, S. He, Self-learning and explainable deep learning network toward the security of artificial intelligence of things, J. Supercomput. 79 (4) (2023) 4436–4467.
[21] P. Long, L. Lu, Q.L. Chen, Y.F. Chen, C.L. Li, X.C. Luo, Intelligent selection of healthcare supply chain mode - an applied research based on artificial intelligence, Front. Public Health 11 (2024) 1310016.
[22] D.J. Jagannath, R.J. Dolly, G.S. Let, J.D. Peter, An IoT enabled smart healthcare system using deep reinforcement learning, Concurr. Comput. Pract. Exp. 34 (28) (2022) e7403.
[23] R. Mussabayev, Optimizing Euclidean distance computation, Mathematics 12 (23) (2024) 3787.
[24] Z.Y. Xu, S. Zhu, S.P. Wen, Finite/fixed-time synchronization of nonidentical chaotic delayed neural networks with Markovian jump and uncertainties via sliding mode control, Int. J. Robust Nonlinear Control 33 (16) (2023) 10064–10082.
[25] Y.H. Xie, Y.Y. Kong, L. Huang, S. Wang, S.Z. Xu, X. Wang, J. Ren, Resource allocation for network slicing in dynamic multi-tenant networks: a deep reinforcement learning approach, Comput. Commun. 195 (2022) 476–486.
[26] A.M. Hilal, L.O. Widaa, F.N. Al-Wesabi, M. Medani, M.A. Hamza, M. Al Duhayyim, Metaheuristic resource allocation strategy for cluster based 6G industrial applications, Comput. Mater. Continua 71 (1) (2021) 667–681.
[27] S.A. Syed, K.S.S. Rani, G.B. Mohammad, G.A. Kumar, K.K. Chennam, R. Jaikumar, Y. Natarajan, K. Srihari, U.B. Nisha, V.P. Sundramurthy, Design of resources allocation in 6G cybertwin technology using the fuzzy neuro model in healthcare systems, J. Healthcare Eng. (2022) 5691203.
[28] S.T. Ahmed, K.K. Patil, S.S. Kumar, R.K. Dhanaraj, S.B. Khan, S. Alzahrani, S. Rani, 6GTelMED: resources recommendation framework on 6G-enabled distributed telemedicine using edge-AI, IEEE Trans. Consum. Electron. 70 (3) (2024) 5524–5532.
[29] P. Bhattacharya, F. Patel, A. Alabdulatif, R. Gupta, S. Tanwar, N. Kumar, R. Sharma, A deep-Q learning scheme for secure spectrum allocation and resource management in 6G environment, IEEE Trans. Netw. Serv. Manag. 19 (4) (2023) 4989–5005.
[30] P. Qin, M. Wang, Z.Y. Cai, R. Ding, X.W. Zhao, Y. Fu, X. Wu, Optimal resource allocation for AGIN 6G: a learning-based three-sided matching approach, IEEE Trans. Netw. Sci. Eng. 11 (2) (2024) 1553–1565.
[31] Z.W. Huang, D.G. Li, J. Cai, H. Lu, Collective reinforcement learning based resource allocation for digital twin service in 6G networks, J. Netw. Comput. Appl. 217 (2023) 103697.